Supplementary Information (SI) for Journal of Materials Chemistry C.

Supporting Information

Raman Spectra of Graphyne-Family: Graphyne, Graphdiyne and Graphtriyne

Kunquan Lin[a,b], Haiming Huang[a,b*], Junyan Zhang[a], Qiuyi Zhong[a], Weiliang Wang[c] and Shaolin Zhang[a,b]

[a] Solid State Physics & Material Research Laboratory, School of Physics and Materials Science, Guangzhou University, Guangzhou 510006, China

[b] Research Center for Advanced Information Materials (CAIM), Huangpu Research and Graduate School of Guangzhou University, Guangzhou 510555, China

[c] School of Physics, Guangdong Province Key Laboratory of Display Material and Technology, Center for Neutron Science and Technology, Sun Yat-sen University, Guangzhou 510275, China

* Corresponding author. E-mail: huanghm@gzhu.edu.cn.

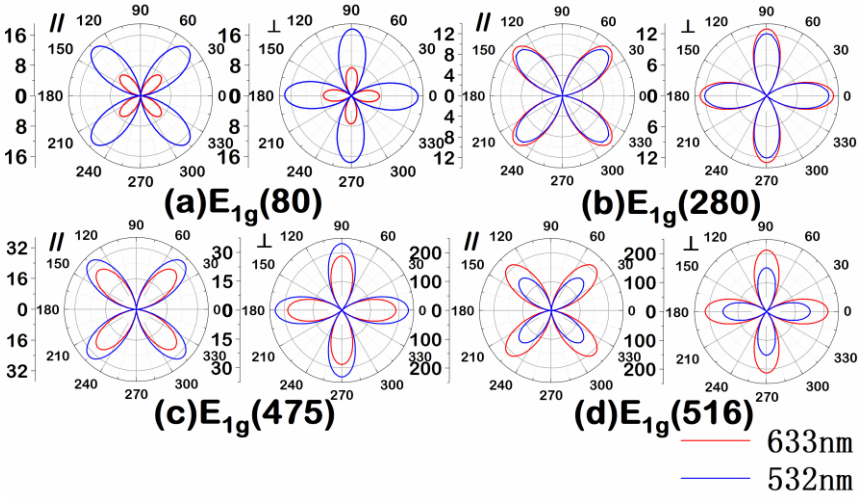

Figure S1 Polar plots of the angular-dependent Raman intensities for (a)E_{1g}(80), (b)E_{1g}(280), (c)E_{1g}(475) and (d)E_{1g}(516) modes of GTY in parallel (left side) and perpendicular (right side) configurations excited by the 633 nm (red) and 532 nm (blue) laser wavelength.

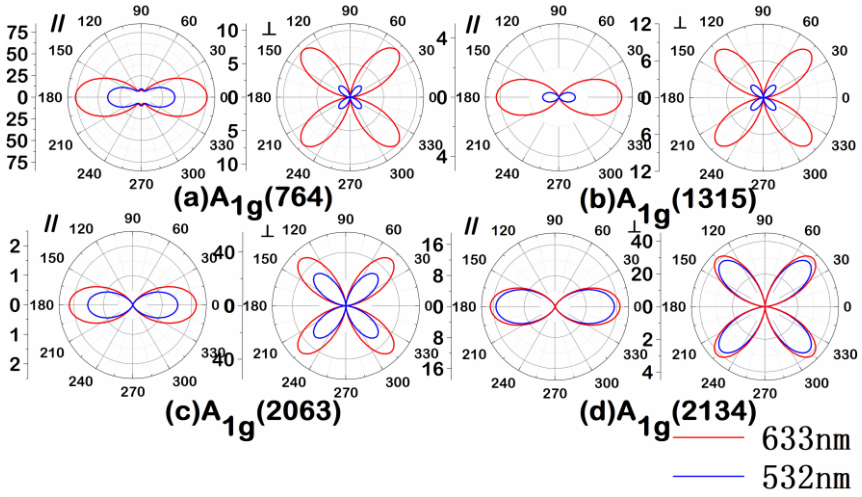

Figure S2 Polar plots of the angular-dependent Raman intensities for (a)A_{1g}(764), (b)A_{1g}(1315), (c)A_{1g}(2063) and (d)A_{1g}(2134) modes of GTY in parallel (left side) and perpendicular (right side) configurations excited by the 633 nm (red) and 532 nm (blue) laser wavelength.

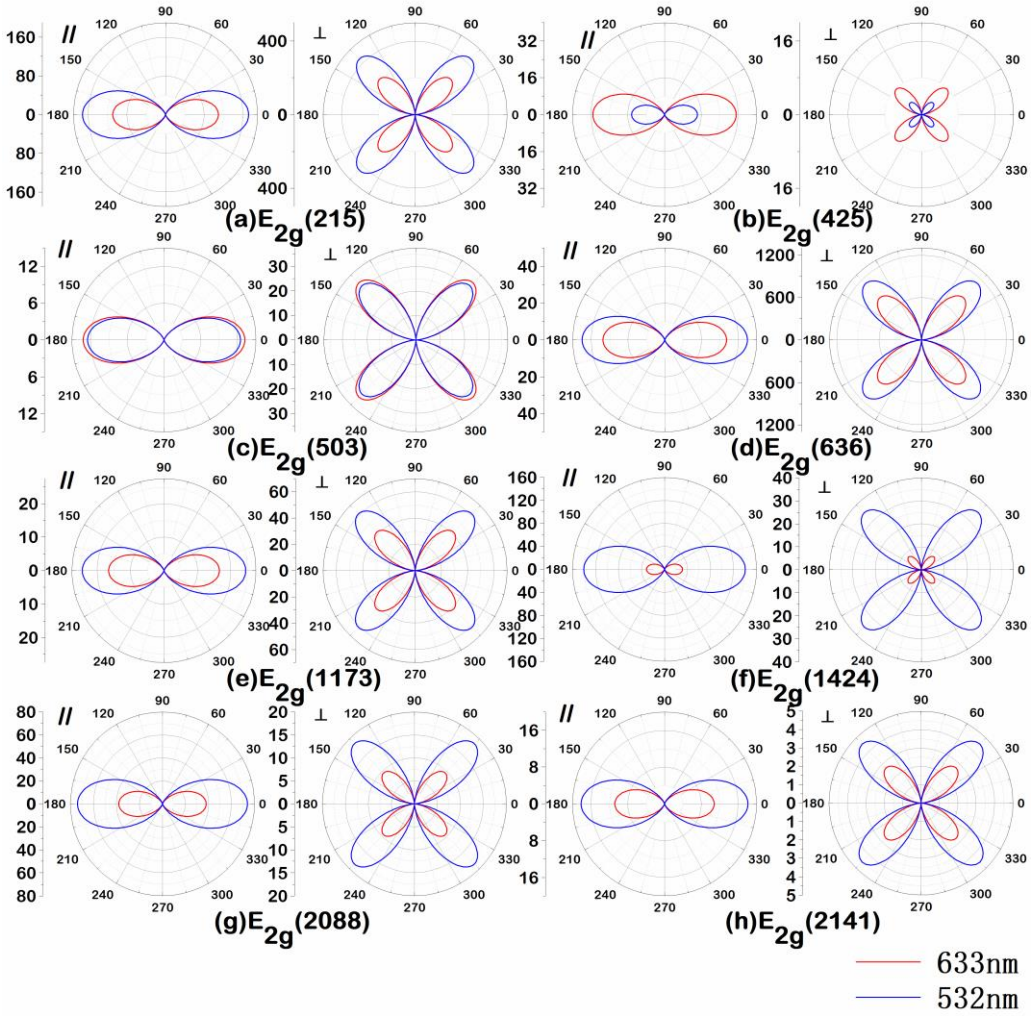

Figure S3 Polar plots of the angular-dependent Raman intensities for (a)E_{2g}(215), (b) E_{2g}(425), (c)E_{2g}(503), (d)E_{2g}(636), (e)E_{2g}(1173), (f)E_{2g}(1424), (g)E_{2g}(2088) and (h)E_{2g}(2141) modes of GTY in parallel (left side) and perpendicular (right side) configurations excited by the 633 nm (red) and 532 nm (blue) laser wavelength.

Table SI. Raman tensor elements a, b, c and d for monolayer GY.

Mode	E_{1g}(230)		E_{1g}(534)					
Laser(nm)	633	532	633	532				
c(arb. units)	$2.24e^{i\times2°}$	$2\ e^{i\times14°}$	$2\ e^{i\times41°}$	$5.8\ e^{i\times19°}$				
Mode	E_{2g}(492)		E_{2g}(921)		E_{2g}(1413)		E_{2g}(2201)	
Laser(nm)	633	532	633	532	633	532	633	532
d(arb. units)	$0.54e^{i\times26°}$	$2.8\ e^{i\times45°}$	$1.36e^{i\times28°}$	$5.7\ e^{i\times41°}$	$124\ e^{-i\times89°}$	$1\ e^{i\times53°}$	$3.9\ e^{-i\times12°}$	$1.27\ e^{i\times70°}$
Mode	A_{1g}(1166)		A_{1g}(2166)					
Laser(nm)	633	532	633	532				
a(arb. units)	$1.6e^{-i\times30°}$	$17\ e^{i\times45°}$	$30\ e^{i\times29°}$	$41\ e^{i\times43°}$				
b(arb. units)	$0.01e^{i\times2°}$	$0.01e^{i\times6°}$	$0.06e^{i\times1°}$	$0.067e^{i\times4°}$				

Table SII. Raman tensor elements a, b, c and d for monolayer GDY.

Mode	E_{1g}(125)		E_{1g}(426)		E_{1g}(525)					
Laser(nm)	633	532	633	532	633	532				
c(arb. units)	$0.14e^{i\times28°}$	$0.29e^{i\times24°}$	$0.05e^{i\times56°}$	$0.14e^{i\times35°}$	$0.17e^{-i\times80°}$	$0.36e^{i\times40°}$				
Mode	E_{2g}(386)		E_{2g}(505)		E_{2g}(759)		E_{2g}(1325)		E_{2g}(1471)	
Laser(nm)	633	532	633	532	633	532	633	532	633	532
d(arb. units)	$1.6e^{-i\times45°}$	$2.11e^{-i\times46°}$	$3.1\ e^{i\times77°}$	$2.5\ e^{i\times81°}$	$3.5\ e^{-i\times88°}$	$2.2\ e^{-i\times74°}$	$18.3\ e^{-i\times63°}$	$12.5e^{-i\times89°}$	$32\ e^{-i\times64°}$	$22\ e^{-i\times62°}$
Mode	E_{2g}(2192)									
Laser(nm)	633	532								
d(arb. units)	$56e^{-i\times62°}$	$30e^{-i\times85°}$								
Mode	A_{1g}(932)		A_{1g}(1433)		A_{1g}(2117)					
Laser(nm)	633	532	633	532	633	532				
a(arb. units)	$12.2\ e^{-i\times62°}$	$9.4\ e^{-i\times86°}$	$22\ e^{-i\times58°}$	$17.2\ e^{i\times83°}$	$62\ e^{i\times59°}$	$49\ e^{i\times87°}$				
b(arb. units)	$0.04\ e^{-i\times0°}$	$0.04\ e^{-i\times0°}$	$1.6\ e^{-i\times0°}$	$1.6\ e^{i\times0°}$	$0.06\ e^{i\times0°}$	$0.06\ e^{i\times0°}$				

Table SIII. Raman tensor elements a, b, c and d for monolayer GTY.

Mode	E_{1g}(80)		E_{1g}(280)		E_{1g}(475)		E_{1g}(516)			
Laser(nm)	633	532	633	532	633	532	633	532		
c(arb. units)	$2.6\ e^{i\times6°}$	$3.1\ e^{i\times22°}$	$2.6\ e^{i\times14°}$	$2.3\ e^{i\times32°}$	$3.7\ e^{i\times49°}$	$3.7\ e^{i\times52°}$	$9.6\ e^{-i\times68°}$	$8\ e^{i\times41°}$		
Mode	E_{2g}(215)		E_{2g}(425)		E_{2g}(503)		E_{2g}(636)		E_{2g}(1173)	
Laser(nm)	633	532	633	532	633	532	633	532	633	532
d(arb. units)	$23.6e^{i\times39°}$	$27.1e^{i\times7°}$	$40\ e^{i\times22°}$	$30\ e^{i\times19°}$	$26\ e^{i\times30°}$	$23\ e^{-i\times4°}$	$41\ e^{i\times15°}$	$44\ e^{i\times19°}$	$29\ e^{-i\times11°}$	$32\ e^{i\times5°}$
Mode	E_{2g}(1424)		E_{2g}(2088)		E_{2g}(2141)					
Laser(nm)	633	532	633	532	633	532				
d(arb. units)	$127e^{i\times27°}$	$245e^{i\times57°}$	$139e^{-i\times51°}$	$178e^{-i\times75°}$	$235\ e^{-i\times23°}$	$279e^{-i\times41°}$				
Mode	A_{1g}(764)		A_{1g}(1315)		A_{1g}(2063)		A_{1g}(2134)			
Laser(nm)	633	532	633	532	633	532	633	532		
a(arb. units)	$197e^{-i\times27°}$	$129\ e^{-i\times18°}$	$466\ e^{-i\times40°}$	$218\ e^{-i\times20°}$	$1048e^{-i\times24°}$	$809e^{-i\times1°}$	$882\ e^{-i\times10°}$	$846\ e^{-i\times1°}$		
b(arb. units)	$65\ e^{i\times0°}$	$65\ e^{i\times0°}$	$1\ e^{i\times0°}$	$1\ e^{i\times0°}$	$62e^{-i\times0°}$	$63\ e^{-i\times0°}$	$2\ e^{-i\times30°}$	$2\ e^{-i\times0°}$		

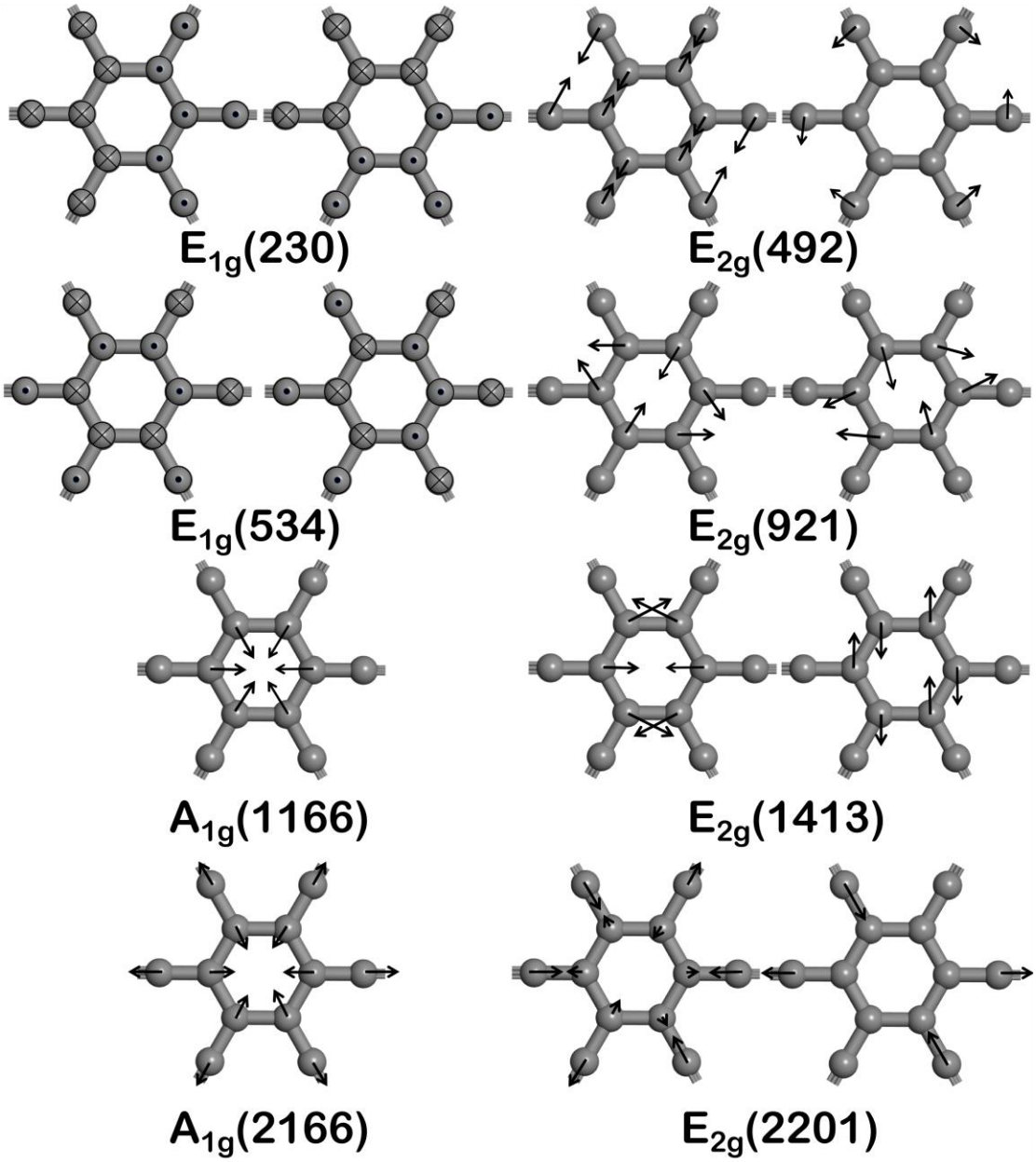

Figure S4 Atomic displacements of the Raman-active modes for GY. The arrow represents the direction of in-plane vibration, while the dot (cross) in the circle represents the vibration direction perpendicular to the paper facing outward (inward).

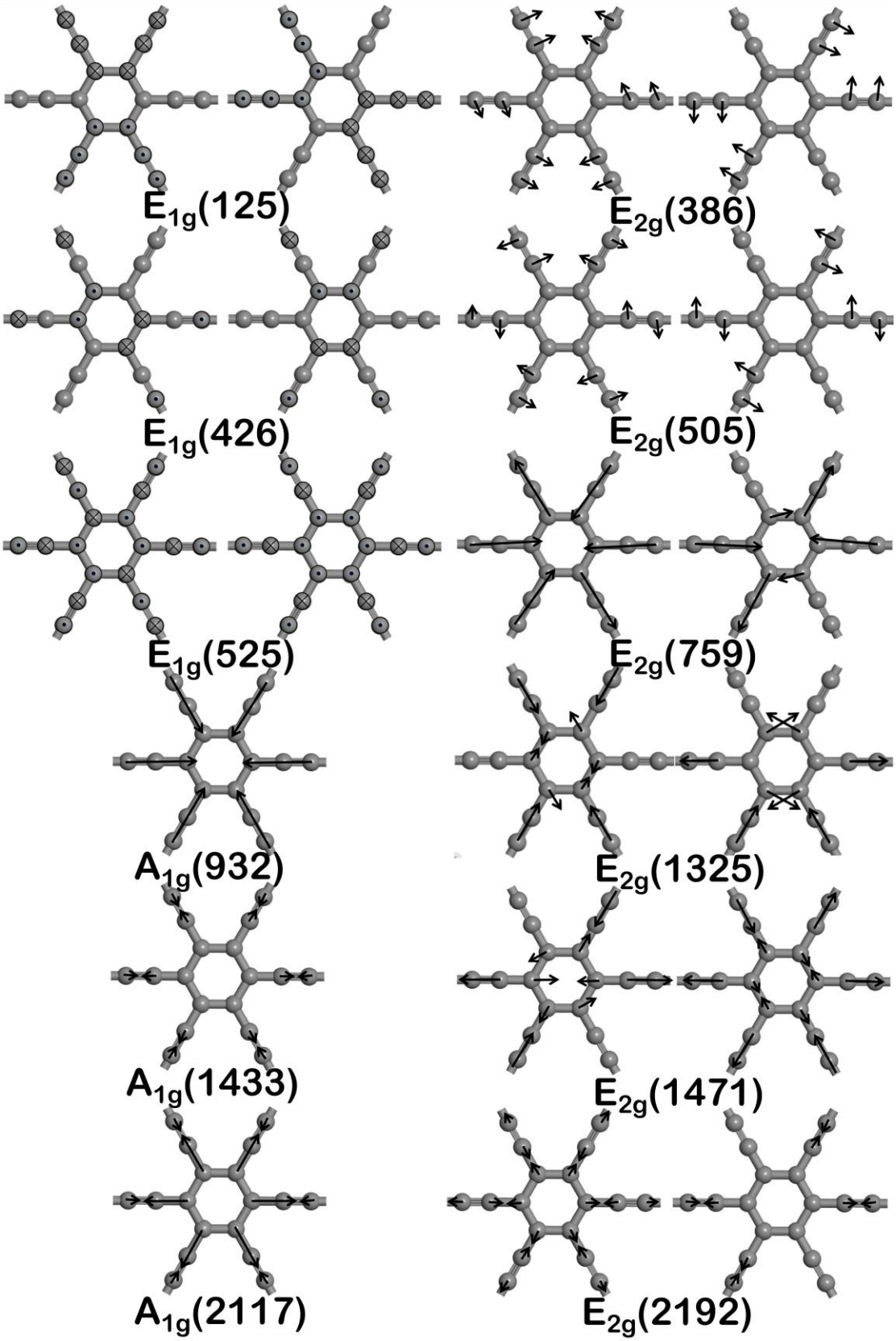

Figure S5 Atomic displacements of the Raman-active modes for GDY. The arrow represents the direction of in-plane vibration, while the dot (cross) in the circle represents the vibration direction perpendicular to the paper facing outward (inward).

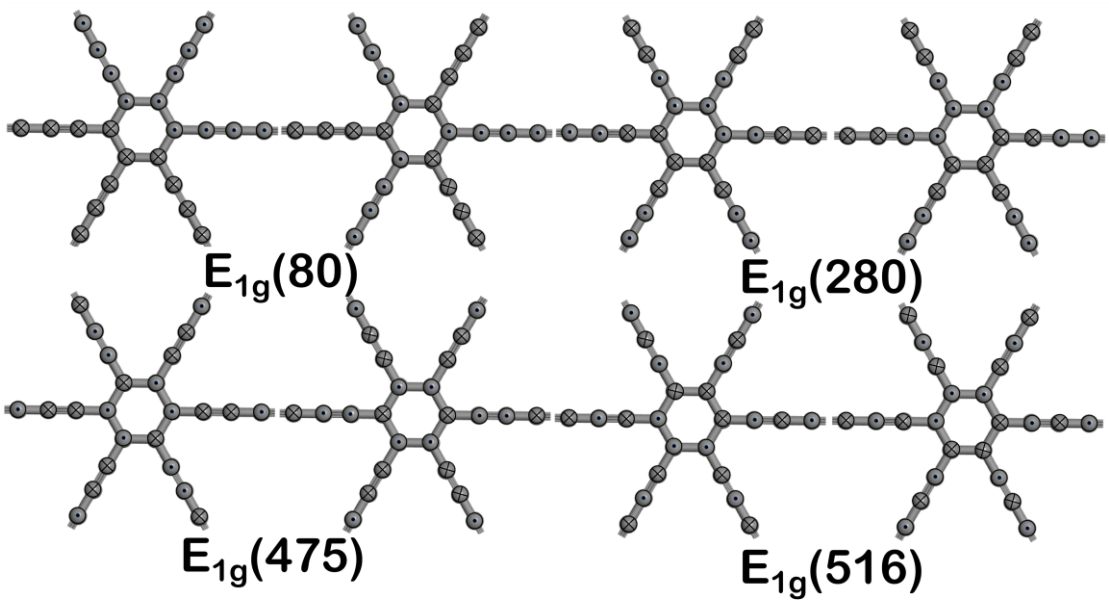

Figure S6 Atomic displacements of the E_{1g} Raman-active modes for GTY. The dot (cross) in the circle represents the vibration direction perpendicular to the paper facing outward (inward).

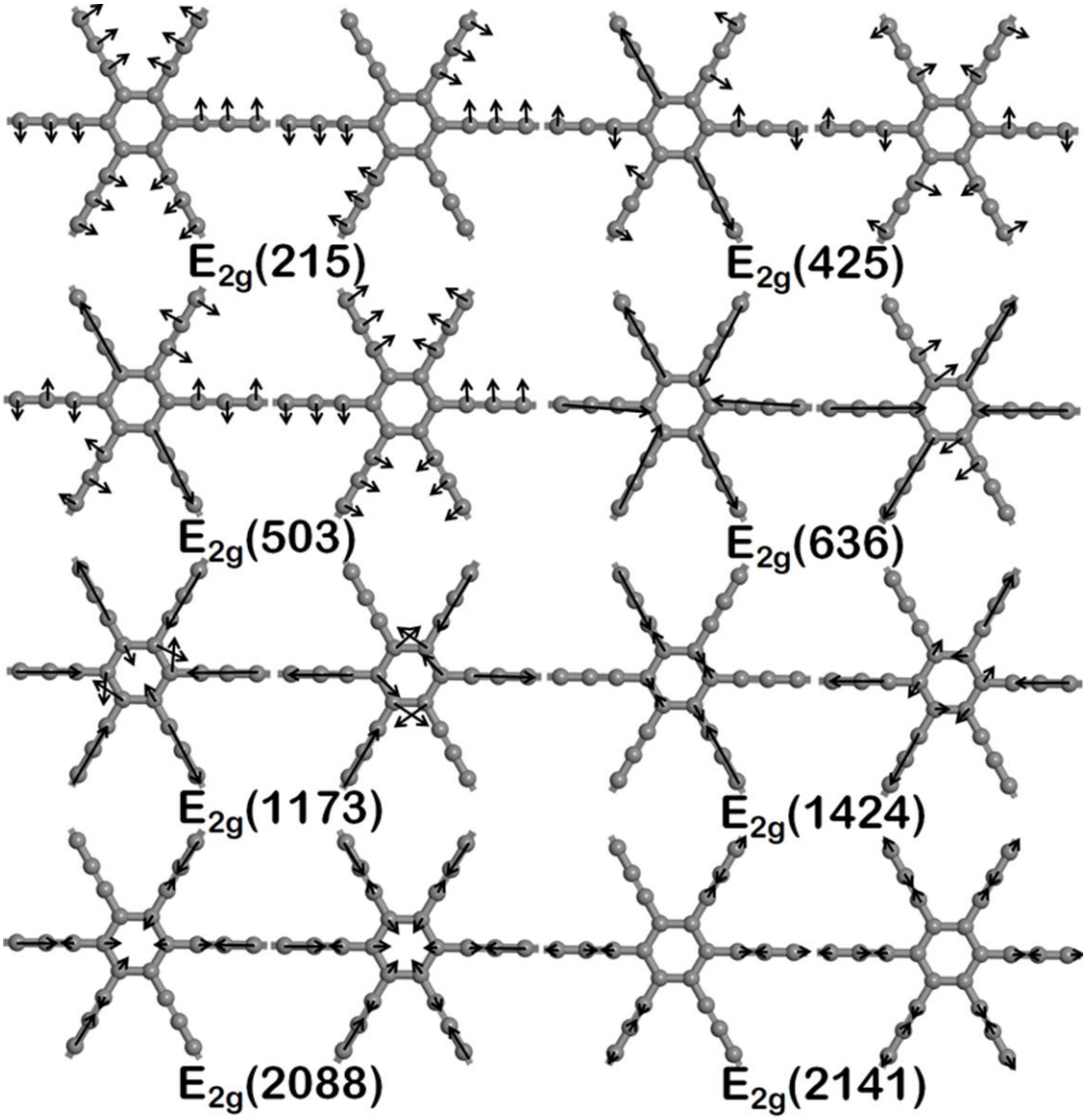

Figure S7 Atomic displacements of the E_{2g} Raman-active modes for GTY. The arrow represents the direction of in-plane vibration.

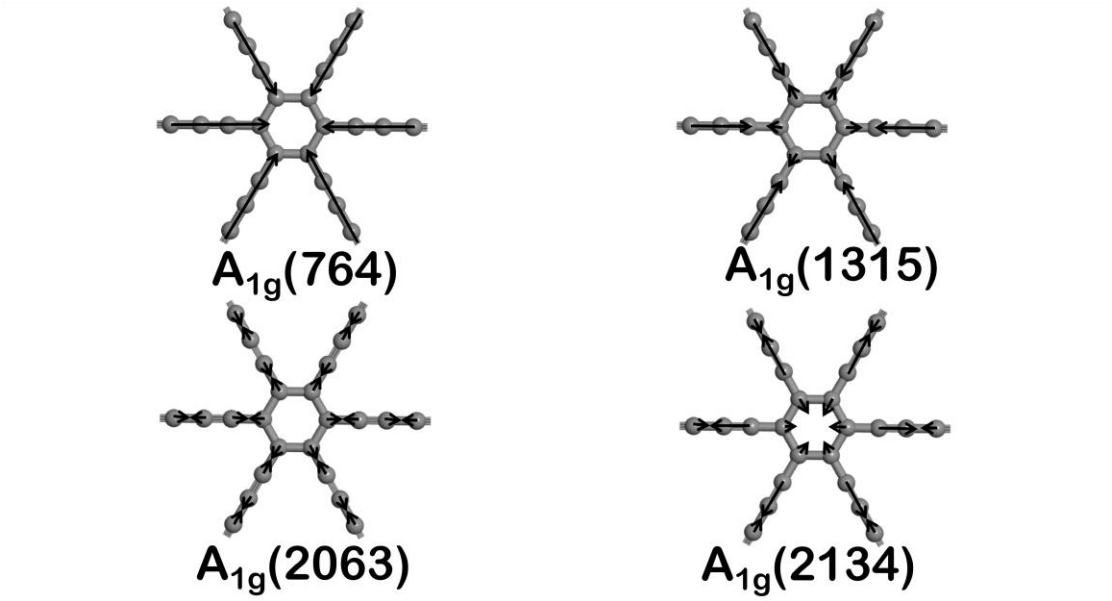

Figure S8 Atomic displacements of the A_{1g} Raman-active modes for GTY. The arrow represents the direction of in-plane vibration.

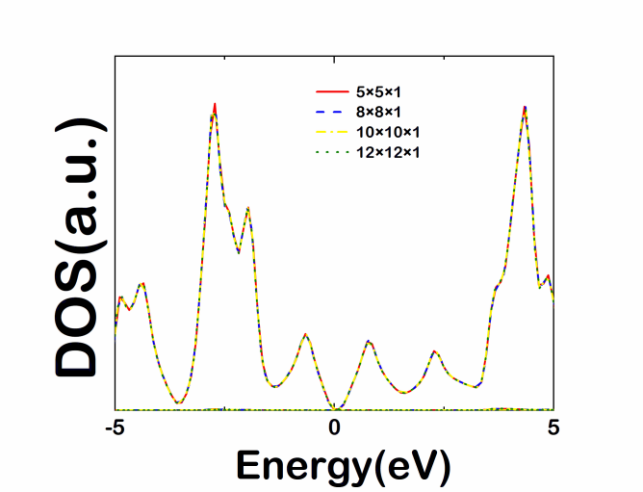

Figure S9 Densities of states of GY by using different Monkhorst-Pack grids of K-points.